



Distributed material density and anisotropy for optimized eigenfrequency of 2D continua

Pedersen, Pauli; Pedersen, Niels Leergaard

Published in:
Structural and Multidisciplinary Optimization

Link to article, DOI:
[10.1007/s00158-014-1196-6](https://doi.org/10.1007/s00158-014-1196-6)

Publication date:
2015

Document Version
Peer reviewed version

[Link back to DTU Orbit](#)

Citation (APA):
Pedersen, P., & Pedersen, N. L. (2015). Distributed material density and anisotropy for optimized eigenfrequency of 2D continua. *Structural and Multidisciplinary Optimization*, 51, 1067-1076.
<https://doi.org/10.1007/s00158-014-1196-6>

General rights

Copyright and moral rights for the publications made accessible in the public portal are retained by the authors and/or other copyright owners and it is a condition of accessing publications that users recognise and abide by the legal requirements associated with these rights.

- Users may download and print one copy of any publication from the public portal for the purpose of private study or research.
- You may not further distribute the material or use it for any profit-making activity or commercial gain
- You may freely distribute the URL identifying the publication in the public portal

If you believe that this document breaches copyright please contact us providing details, and we will remove access to the work immediately and investigate your claim.

Distributed material density and anisotropy for optimized eigenfrequency of 2D continua

Pauli Pedersen and Niels L. Pedersen

Abstract Key words Eigenfrequency sensitivity - optimality criterion - recursive optimization - free material - constitutive components

A practical approach to optimize a continuum/structural eigenfrequency is presented, including design of the distribution of material anisotropy. This is often termed free material optimization (FMO). An important aspect is the separation of the overall material distribution from the local design of constitutive matrices, i.e., the design of the local anisotropy.

For a finite element (FE) model the amount of element material is determined by a traditional optimality criterion (OC) approach. In this respect the major value of the present formulation is the derivation of simple eigenfrequency gradients with respect to material density and from this values of the element OC. Each factor of this expression has a physical interpretation. Stated alternatively, the optimization problem of material distribution is converted into a problem of determining a design of uniform OC values.

The constitutive matrices are described by non-dimensional matrices with unity norms of trace and Frobenius, and thus this part of the optimized design has no influence on the mass distribution. Gradients of eigenfrequency with respect to the components of these non-dimensional constitutive matrices are therefore simplified, and an additional optimization criterion shows that the optimized redesign of anisotropy are described directly by the element strains.

The fact that all components of an optimal constitutive matrix are expressed by the components of a strain state, imply a reduced number of independent components of an optimal constitutive matrix. For 3D problems from 21 to 6 parameters, for 2D from 6 to 3 parameters, and for axisymmetric problems from 10 to 4 parameters.

Received: date / Revised version: date

Pauli Pedersen and Niels L. Pedersen

Department of Mechanical Engineering,
Solid Mechanics, Technical University of Denmark
Nils Koppels Allè, B 404, DK-2800 Kgs.Lyngby, Denmark
e-mail: pauli@mek.dtu.dk and e-mail: nlp@mek.dtu.dk

1 Introduction

Early optimal design of beams in order to maximize the first eigenfrequency were based on differential equation approaches, see Niordson (1965). Plates and other structural models then followed, see review by Grandhi (1993). The finite element (FE) approach of the present paper relates to a decided design domain, where the material densities of the elements are the design variables, and in addition the element constitutive components are subjected to design. This is termed free material optimization (FMO), often applied to static problems. In research related to semi-definite programming, eigenvalue constraints are also included, see Stingl et al. (2009).

The formulation and the theoretical results are valid for a large class of problems: 1D, 2D or 3D - numerical or analytical - continuum or structure. The limitations are set by a model described by symmetric, positive definite matrices for stiffness as well as for mass (for the system model including the assumed boundary conditions).

The present structural optimization may be divided into four steps, performed successively to obtain a redesign. First step is analysis of a current design, which is obtained by the standard procedure of subspace iteration. Second step is sensitivity analysis to obtain gradients of the eigenfrequencies with respect to element material density. A simple explicit formula for this is derived and presented. This is found to be important, due to its generality and presented by factors with direct physical interpretation. The third step is a redesign of material densities based on an optimality criterion, closely related to the gradients from sensitivity analysis. The numerical approach for solution is heuristic, earlier applied with good experience from other problem such as shape optimization for eigenfrequency control, see Pedersen and Pedersen (2005).

The fourth step immediately seems complicated, i.e., how to redesign each element constitutive matrix advantageously? A new optimality criterion for this step allows to redesign directly from the strain field corresponding to the current eigenmode. This is performed, automatically satisfying normalized, non-dimensional constitutive matrices with unit norms of trace and Frobenius. Mathematical proof of this is included. The fact that three strain components in 2D (6 in 3D) describe the anisotropy, means that not any constitutive matrix (6 components in 2D, 21 in 3D) can satisfy the optimality criterion,

exemplified by that only zero Poisson's ratio for isotropy is possible.

The layout of the paper is as follows. Analysis and sensitivity analysis are described in Section 2. In Section 3 the problem of material distribution to maximize the first eigenfrequency is stated with non-dimensional design parameters ρ_e for the elements, size constraints $0 < \rho_{\min} < \rho_e < \rho_{\max} \leq 1$ and a constraint on the amount of material $V = \sum_e \rho_e V_e$, where V_e is the volume of element e . In Section 4 the problem of design of constitutive matrices is presented in detail, i.e., the determination of the local anisotropy. Constraints that ensure symmetric, positive definite matrices are stated and furthermore these matrices are all normalized to unit norm of trace as well as of Frobenius norm. From a derived optimality criterion it is proved that these constraints are always satisfied. The case of semi-positive is numerically accounted for by always keeping a small amount of isotropy, just like material density should never vanish, say by $\rho_e \geq 0.01$.

In Section 5 two examples are chosen to verify the presented theory and applied procedure. With the actual design domains and boundary conditions, these examples may be seen as 2D versions of beam like models. The cantilever model illustrate how a fixed design domain at the free tip, force a more meaningful solution. In general robust convergence is found. The second example of a beam-bridge model is designed as a full model. This example illustrate mode switching between symmetric and antisymmetric modes. Even if only the first eigenfrequency is of interest, the subspace iteration is set to determine several eigenmodes, to get information on the frequency spectrum closest to given shift value (here zero).

2

Analysis and sensitivity analysis

For a given continuum/structure, analysis by subspace iteration, gives a series of eigenmodes, described individually by an eigenvector $\{D\}$, orthogonal to the other determined eigenvectors and normalized so that the specific kinetic energy $T = 1$. With this normalization of the eigenvector, the specific elastic energy U is numerically equal to the eigenvalue ω^2 , i.e., for the numerical values $U = \omega^2 = \omega^2 T$, where T and U are the time independent amplitudes.

Let us assume an eigenvalue problem described by the symmetric positive definite stiffness matrix $[S]$ and the symmetric positive definite mass matrix $[M]$. An assumed simple (non-multiple) eigenvector is $\{D\}$ from which the system specific elastic energy (twice the strain energy) is U and this energy may be accumulated from element energies U_e . Analogously the system specific kinetic energy T may be accumulated from element specific kinetic energies T_e .

In the sensitivity analysis we use the following results from subspace analysis

$$\omega^2, U_e, T_e \text{ with } \{D\} \text{ normalized such that} \\ U = \sum U_e = \omega^2, \quad T = \sum T_e = 1, \quad \omega^2 = U/T \quad (1)$$

where U/T is the Rayleigh quotient. Further we define element Rayleigh quotients U_e/T_e , that in a somewhat loose notation are termed element squared frequencies

$$\omega_e^2 = \frac{U_e}{T_e} = \frac{\{D_e\}^T [S_e] \{D_e\}}{\{D_e\}^T [M_e] \{D_e\}} \quad (2)$$

As proved below in Section 2.1 the sensitivity of squared eigenfrequency ω^2 with respect to relative material density $0 < \rho_e \leq 1$ in element e is

$$\frac{\partial \omega^2}{\partial \rho_e} = \frac{T_e}{T \rho_e} (\omega_e^2 - \omega^2) \quad (3)$$

This simple result with direct physical interpretation of each factor is valid for a general model described by positive definite, symmetric stiffness and mass matrices at the system level, for continuum as well as structure, analytical described as well numerical discretized. The gradient result (3) is for stiffness and mass linear depending on ρ_e as proved in Section 2.1.

The element specific elastic energy U_e , in linear displacements elements e follows directly from a displacement mode that give a constant elastic energy density u_e and thus

$$U_e = u_e \rho_e V_e \quad (4)$$

where V_e is the geometric reference volume of the element e . Alternative evaluation of U_e must be derived as the nominator in (2) for elements without constant energy density. The element specific kinetic energy T_e in element e need to be determined from the element displacement mode $\{D_e\}$ and a consistent mass matrix with no coupling between x -, y -directions. The specific kinetic energy can then be divided into two terms, that exemplified for the x -direction is

$$(T_e)_x = \frac{m_e}{12} \{D_e\}_x^T \begin{bmatrix} 2 & 1 & 1 \\ 1 & 2 & 1 \\ 1 & 1 & 2 \end{bmatrix} \{D_e\}_x \quad \text{with } m_e = \rho_M \rho_e V_e \quad (5)$$

where m_e is the mass of element e . The mass density with physical dimension kg/m^3 is termed ρ_M to distinguish from the non-dimensional material volume densities, that traditionally has the notation ρ_e . From (5) a rather simple analytical expression follows. In general for a linear displacement FE model, the numerical calculations may be based on explicit formulas without numerical integration.

2.1

Derivation of eigenfrequency gradients

For linear stiffness interpolation, the expression (3) is derived in the following. For extension to non-linear interpolation functions see Pedersen and Pedersen (2012). The design parameters ρ_e are assumed to be local, positive non-dimensional quantities in the interval $0 < \rho_e \leq 1$. We here assume both

the element stiffness matrix $[S_e]$ and the element mass matrix $[M_e]$ to be proportional to ρ_e , i.e.,

$$[S_e] = \rho_e [S_e], \quad [M_e] = \rho_e [M_e] \quad (6)$$

with both $[S_e]$ and $[M_e]$ independent of design.

The gradient $\partial\omega^2/\partial\rho_e = \partial(U/T)/\partial\rho_e$ is determined at the element level. To avoid extended indexing a hat notation is introduced by

$$\widehat{\frac{\partial(\cdot)}{\partial\rho_e}} = \left(\frac{\partial(\cdot)}{\partial\rho_e} \right)_{\text{fixed displacement}} = \left(\frac{\partial(\cdot)}{\partial\rho_e} \right)_{\text{fixed strains}} \quad (7)$$

and with this short notation the gradient is determined, finally at the element level

$$\begin{aligned} \frac{\partial\omega^2}{\partial\rho_e} &= \frac{\partial\omega^2}{\partial\{D\}} \frac{\partial\{D\}}{\partial\rho_e} + \frac{\widehat{\partial\omega^2}}{\partial\rho_e} = \frac{1}{T^2} \left(\widehat{\frac{\partial U}{\partial\rho_e}} T - \widehat{\frac{\partial T}{\partial\rho_e}} U \right) \\ &= \frac{1}{T} \left(\widehat{\frac{\partial U_e}{\partial\rho_e}} - \omega^2 \widehat{\frac{\partial T_e}{\partial\rho_e}} \right) \end{aligned} \quad (8)$$

because $\partial\omega^2/\partial\{D\} = \partial(U/T)/\partial\{D\} = \{0\}^T$. This result, based on the assumption of symmetric matrices $[S]$ and $[M]$, is presented in Wittrick (1962) with further reference to Jacobi (1846). Inserting the assumptions of linear dependency $\widehat{\partial U_e/\partial\rho_e} = U_e/\rho_e$ and $\widehat{\partial T_e/\partial\rho_e} = T_e/\rho_e$ gives the local result where the gradient is expressed by local energies

$$\frac{\partial\omega^2}{\partial\rho_e} = \frac{1}{T\rho_e} (U_e - \omega^2 T_e) = \frac{T_e}{T\rho_e} (\omega_e^2 - \omega^2) \quad (9)$$

The gradient is proportional to the difference between the local ratio of energies (local Rayleigh quotient or termed local squared frequency) ω_e^2 and the system squared eigenfrequency ω^2 .

From expression (9) follows directly the sign of the gradient as all T_e, T, ρ_e are non-negative quantities

$$\begin{aligned} \frac{\partial\omega^2}{\partial\rho_e} &> 0 \quad \text{for } \omega_e^2 > \omega^2, \quad \frac{\partial\omega^2}{\partial\rho_e} < 0 \quad \text{for } \omega_e^2 < \omega^2, \\ \frac{\partial\omega^2}{\partial\rho_e} &= 0 \quad \text{for } \omega_e^2 = \omega^2 \end{aligned} \quad (10)$$

To increase the frequency of the continuum/structure we increase ρ_e for $\omega_e^2 > \omega^2$ and decrease ρ_e for $\omega_e^2 < \omega^2$. A design change may be limited by the active constraint for material as stated in (11) and by the fact that sensitivity analysis will change when changing the design. The solution to these problems is obtained by the heuristic iterative optimization procedure, shortly described in Section 3.

3

A density optimization problem and its optimality criterion

We study the optimization problem to maximize an eigenvalue (assumed single and being the first one) ω^2 for a given

amount of material, specified by the volume V . We assume this volume constraint to be active and state the problem with non-dimensional densities ρ_e as design variables

$$\begin{aligned} &\text{Maximize } \omega^2 \quad (\text{objective}) \\ &\text{for all densities } 0 < \rho_{\min} \leq \rho_e \leq \rho_{\max} \leq 1 \quad (\text{size limits}) \\ &\text{and } g = \sum \rho_e V_e - V = 0 \quad (\text{active constraint}) \end{aligned} \quad (11)$$

The optimality criterion for material distribution OC_m with only a single, active constraint is proportionality between the gradients of the objective and the gradients of the constraint, i.e.,

$$\frac{\partial\omega^2}{\partial\rho_e} = \lambda \frac{\partial g}{\partial\rho_e} = \lambda V_e \Rightarrow \lambda_e = \frac{1}{V_e} \frac{\partial\omega^2}{\partial\rho_e} = \lambda \quad (12)$$

with the same value $\lambda_e = \lambda$ for all elements (sub-domains) e having an active design parameter ρ_e where $\rho_{\min} < \rho_e < \rho_{\max}$. For a given design a number of different values λ_e result, and we want to change the design in order for these values to become more equal for the active design elements (resulting in the unknown Lagrange multiplier λ). With linear stiffness interpolation the gradient $\partial\omega^2/\partial\rho_e$ is given in (9) and the optimality criterion for distribution of material density OC_m is

$$\lambda_e = \frac{T_e}{T} \frac{1}{\rho_e V_e} (\omega_e^2 - \omega^2) = \lambda \quad (13)$$

3.1

Possible heuristic numerical procedure

The optimization problem (11) is by the OC_m (12) converted to a problem of finding a continuum of best possible uniformity of the values of the local OC_m (λ_e). Size limits and the active material volume constraint in (11) normally do not allow for satisfying the OC_m everywhere. Iteratively the active size constraints are fulfilled.

A heuristic recursive procedure for optimization based on (13) is separated according to the sign of the gradients (sign of $(\omega_e^2 - \omega^2)$). The redesign of the ρ_e follows

$$\begin{aligned} &\text{For positive gradients } (\omega_e^2 - \omega^2 > 0) \\ &(\rho_e)_{\text{new}} = (\rho_e)_{\text{current}} (1 + 4.0 \lambda_e / \lambda_{\max})^q \eta \\ &\text{For negative gradients } (\omega_e^2 - \omega^2 < 0) \\ &(\rho_e)_{\text{new}} = (\rho_e)_{\text{current}} (1 - 0.8 \lambda_e / \lambda_{\min})^q \eta \end{aligned} \quad (14)$$

where the values of $\lambda_{\min} < 0, \lambda_{\max} > 0$ are determined during the evaluation of the gradients. The specific values for control parameters in (14), 4.0, 0.8, $q = 0.8$, are chosen from experience, acting as a kind of move-limits and influence the number of recursive redesigns (number of eigenvalue analysis). The iteratively (without FE analysis) determined volume correction factor η relate to the fact that the densities at the limits ρ_{\min} or ρ_{\max} are not known in advance. Factor η strictly keep the specified volume by inner iteration where the ρ_e at

the size limits are localized. This is described in detail in Pedersen and Pedersen (2012). The value $q = 0.8$ of the power also limits the change of ρ_e in one redesign, and such a power (also with a lower value) is often applied for similar recursive procedures. The procedure is applied in the following examples, and have earlier been applied with success to different other problems.

4

Redesign of components for normalized constitutive matrices

The separation of the local constitutive matrix $[L_e]$ is

$$[L_e] = \rho_e E_0 [\tilde{L}_e] \\ = \rho_e E_0 \begin{bmatrix} (\tilde{L}_{1111})_e & (\tilde{L}_{1122})_e & \sqrt{2}(\tilde{L}_{1112})_e \\ (\tilde{L}_{1122})_e & (\tilde{L}_{2222})_e & \sqrt{2}(\tilde{L}_{2212})_e \\ \sqrt{2}(\tilde{L}_{1112})_e & \sqrt{2}(\tilde{L}_{2212})_e & 2(\tilde{L}_{1212})_e \end{bmatrix} \quad (15)$$

where $[\tilde{L}_e]$ is a non-dimensional matrix of unit norm, i.e., a non-dimensional description of the material anisotropy. The discussion of this matrix is here of primary interest as the optimal determination of ρ_e is described in Section 3. The dimensional modulus E_0 is a fixed constant. The problem of optimizing the first eigenfrequency by redesign of the anisotropy of element e is stated

Maximize ω^2 (objective)

by redesign of non-dimensional constitutive components

\tilde{L}_{ijkl} (design parameters subject to unity Frobenius norm)

$h = (\text{Frobenius}([\tilde{L}])^2 - 1 = 0$ (active constraints) (16)

The optimality criterion corresponding to this problem is termed OC_a . With only a single, active constraint the criterion is again proportionality between the gradients of the objective and the gradients of the constraint, i.e.,

$$\frac{\partial \omega^2}{\partial (\tilde{L}_{ijkl})_e} = \Lambda \frac{\partial h}{\partial (\tilde{L}_{ijkl})_e} \quad (17)$$

for which the involved gradients are then derived.

4.1

Gradients and resulting optimality criterion

The local gradient of the Rayleigh quotient with respect to the components of the local constitutive matrix is more simple than (9), because the mass distribution is unchanged (T an T_e unchanged), here with hat notation as an alternative to

extended index

$$\begin{aligned} \frac{\partial \omega^2}{\partial (\tilde{L}_{ijkl})_e} &= \frac{\partial (U/T)}{\partial (\tilde{L}_{ijkl})_e} = \frac{\partial (\widehat{U/T})}{\partial (\tilde{L}_{ijkl})_e} = \frac{\partial (\widehat{U_e/T_e})}{\partial (\tilde{L}_{ijkl})_e} \\ &= \frac{1}{T_e} \frac{\partial \widehat{U_e}}{\partial (\tilde{L}_{ijkl})_e} = \frac{\rho_e V_e}{T_e} \frac{\partial \widehat{u_e}}{\partial (\tilde{L}_{ijkl})_e} \end{aligned} \quad (18)$$

with fixed strains in $u_e = \{\epsilon\}_e^T [\tilde{L}]_e \{\epsilon\}_e$

From the final relation in (18) then follows

$$\begin{aligned} \frac{\partial \omega^2}{\partial (\tilde{L}_{1111})_e} &= \frac{\rho_e V_e}{T_e} (\epsilon_{11}\epsilon_{11})_e, \quad \frac{\partial \omega^2}{\partial (\tilde{L}_{2222})_e} = \frac{\rho_e V_e}{T_e} (\epsilon_{22}\epsilon_{22})_e, \\ \frac{\partial \omega^2}{\partial (\tilde{L}_{1212})_e} &= 4 \frac{\rho_e V_e}{T_e} (\epsilon_{12}\epsilon_{12})_e, \quad \frac{\partial \omega^2}{\partial (\tilde{L}_{1122})_e} = 2 \frac{\rho_e V_e}{T_e} \epsilon_{11}\epsilon_{22})_e, \\ \frac{\partial \omega^2}{\partial (\tilde{L}_{1112})_e} &= 4 \frac{\rho_e V_e}{T_e} (\epsilon_{11}\epsilon_{12})_e, \quad \frac{\partial \omega^2}{\partial (\tilde{L}_{2212})_e} = 4 \frac{\rho_e V_e}{T_e} (\epsilon_{22}\epsilon_{12})_e \end{aligned} \quad (19)$$

The gradients of the constraint $h = F^2 - 1 = 0$ are directly

$$\begin{aligned} \frac{\partial h}{\partial (\tilde{L}_{1111})_e} &= 2(\tilde{L}_{1111})_e, \quad \frac{\partial h}{\partial (\tilde{L}_{2222})_e} = 2(\tilde{L}_{2222})_e, \\ \frac{\partial h}{\partial (\tilde{L}_{1212})_e} &= 8(\tilde{L}_{1212})_e, \quad \frac{\partial h}{\partial (\tilde{L}_{1122})_e} = 4(\tilde{L}_{1122})_e, \\ \frac{\partial h}{\partial (\tilde{L}_{1112})_e} &= 8(\tilde{L}_{1112})_e, \quad \frac{\partial h}{\partial (\tilde{L}_{2212})_e} = 8(\tilde{L}_{2212})_e \end{aligned} \quad (20)$$

Comparing (19) and (20) it is seen that the optimality criterion OC_a for 2D plane problems is satisfied for

$$(\tilde{L}_{ijkl})_e = (\epsilon_{ij}\epsilon_{kl}/(\epsilon_{11}^2 + \epsilon_{22}^2 + 2\epsilon_{12}^2))_e \quad (21)$$

4.2

Proof of unit norms

As seen from (21) $[\tilde{L}_e] = \{\alpha\}\{\alpha\}^T$ is described by such a dyadic product. Then by definitions of trace and Frobenius norms follows, that the values of trace and Frobenius norms are always equal and $[\tilde{L}_e]$ is semi-positive definite.

$$\text{Trace}[\tilde{L}_e] = \text{Frobenius}[\tilde{L}_e] = \{\alpha\}^T \{\alpha\}$$

where $\{\alpha\}^T \{\alpha\} > 0$ for $\{\alpha\} \neq \{0\}$ (22)

Omitting the index e for element, point or domain we proceed the discussion of the obtained constitutive matrix as described directly by the corresponding strain state. Although a constitutive matrix is not necessary obtainable as a dyadic product, this will be the case for the optimal constitutive matrix, where the important result in 2D plane problems with normalization to unit norms is

$$\begin{aligned} [\tilde{L}] &= \{\alpha\}\{\alpha\}^T \text{ with} \\ \{\alpha\}^T &= \{\epsilon_{11} \quad \epsilon_{22} \quad \sqrt{2}\epsilon_{12}\}/\sqrt{\epsilon_{11}^2 + \epsilon_{22}^2 + 2\epsilon_{12}^2} \end{aligned} \quad (23)$$

That the optimal constitutive matrix of unit norms in 2D is described by only three parameters (the strain components) limits the possibilities for a matrix with normally up to 6 independent parameters. An example is that an isotropic $[\tilde{L}]$ is only possible with zero Poisson's ratio and for this case $\{\alpha\}^T = \{1 \ 1 \ 1\}/\sqrt{3}$.

Numerically the rate of change of the constitutive matrices are in each redesign limited by a non-dimensional step parameter $0 \leq \beta \leq 1$ similar to the design approach for strength optimization in Pedersen and Pedersen (2013) where $\beta = 0.5$ and $\beta = 0.1$ were used, i.e.,

$$[\tilde{L}]_{\text{new}} = \beta[\tilde{L}]_{\text{from (23)}} + (1 - \beta)[\tilde{L}]_{\text{old}} \quad (24)$$

The design approach is initiated with $[\tilde{L}]_0 = [I]/3$, i.e., zero Poisson's ratio isotropic material, non-dimensional and normalized. It is concluded that for a given strain state the optimized non-dimensional constitutive matrix is known with unit trace and Frobenius norm. Note, that with initial positive definite $[\tilde{L}]$ it will for $\beta < 1$ stay positive definite through the redesign iterations. For the present eigenfrequency problems, the numerical value $\beta = 0.2$ is applied, and even with this rather low value fast convergence is obtained.

5 Two design examples

Two examples, each with four different amounts of material, are presented. First a cantilever problem where a fixed design domain is included so that a degenerated optimized design is avoided. The influence of the amount of material is illustrated and the redesign history is shown with and without redesign of anisotropy. The increase in the value of the first eigenfrequency with a factor up to 2.2 by only redesign of material distribution, while with including optimized constitutive matrices then with a factor up to 3.5.

The second example is a simply supported beam-bridge with no fixed design domain. To some extent modeling with assumed symmetric eigenmode is possible for half the model, but the possibility of mode switching from symmetric mode to antisymmetric mode for extended redesign is illustrate. Figures show the history of resulting eigenfrequencies for four different problems with amount of material set to 20%, 40%, 60% and 80% of full amount of material, all with uniform initial designs and this means that the four initial problems have identical eigenfrequencies (in the figures normalized to unity).

5.1 Cantilever with fixed tip design

Figure 1 shows the dimensions and data applied for this example, and the 0.4m close to the tip is fixed to the initial value of the density. The mass and stiffness for this domain is thus different for the treated cases of 20%, 40%, 60% and 80% material, but without influence on the response of the initial

uniform designs. The specific FE model has 16384 elements ($128 \times 32 \times 4$) and 16706 dof.

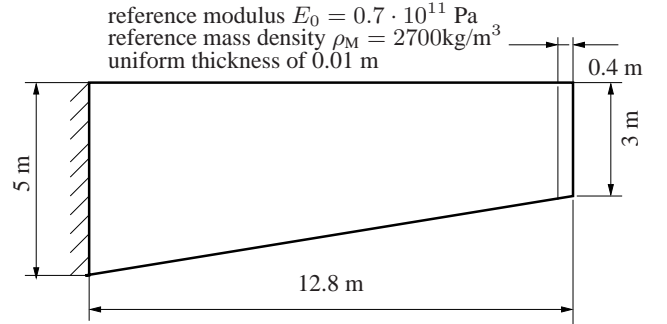


Fig. 1 Data for the cantilever problem with fixed design near the free tip (0.4m).

With focus on the case of 20% material Figure 2 shows the history of results for two different redesign iterations. The dotted curve corresponds to redesigns of both density and anisotropy already from the first redesign, and convergence in 10 redesigns is observed. The full curve also give information about the result after 10 iterations where anisotropy is not optimized, and thus corresponds to a more traditional optimization. In this manner the essential importance of anisotropy is shown.

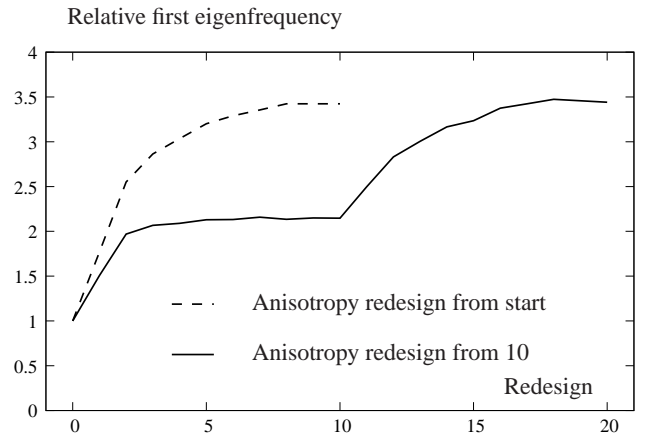


Fig. 2 Iteration histories for the cantilever problem with 20% material. Full line: only anisotropy redesign from redesign number 10. Broken line: anisotropy redesign from redesign number 0.

The initial design, illustrated in Figure 3a is uniform material density (here ρ_e all equal to 0.2). At the tip domain this is not changed. Figure 3b shows the distribution of values of optimality criterion for material distribution OC_m for the initial design in 3a. The positive as well as negative values illustrate that a better material distribution can be obtained by redesign.

After 10 redesigns of only material density, the first eigenfrequency is increased with a factor close to 2.2, and Figure 3c shows the optimized material distribution, when isotropy is kept. Figure 3d shows the distribution of OC_m values for the optimized design in 3c. Note, that these OC_m values are

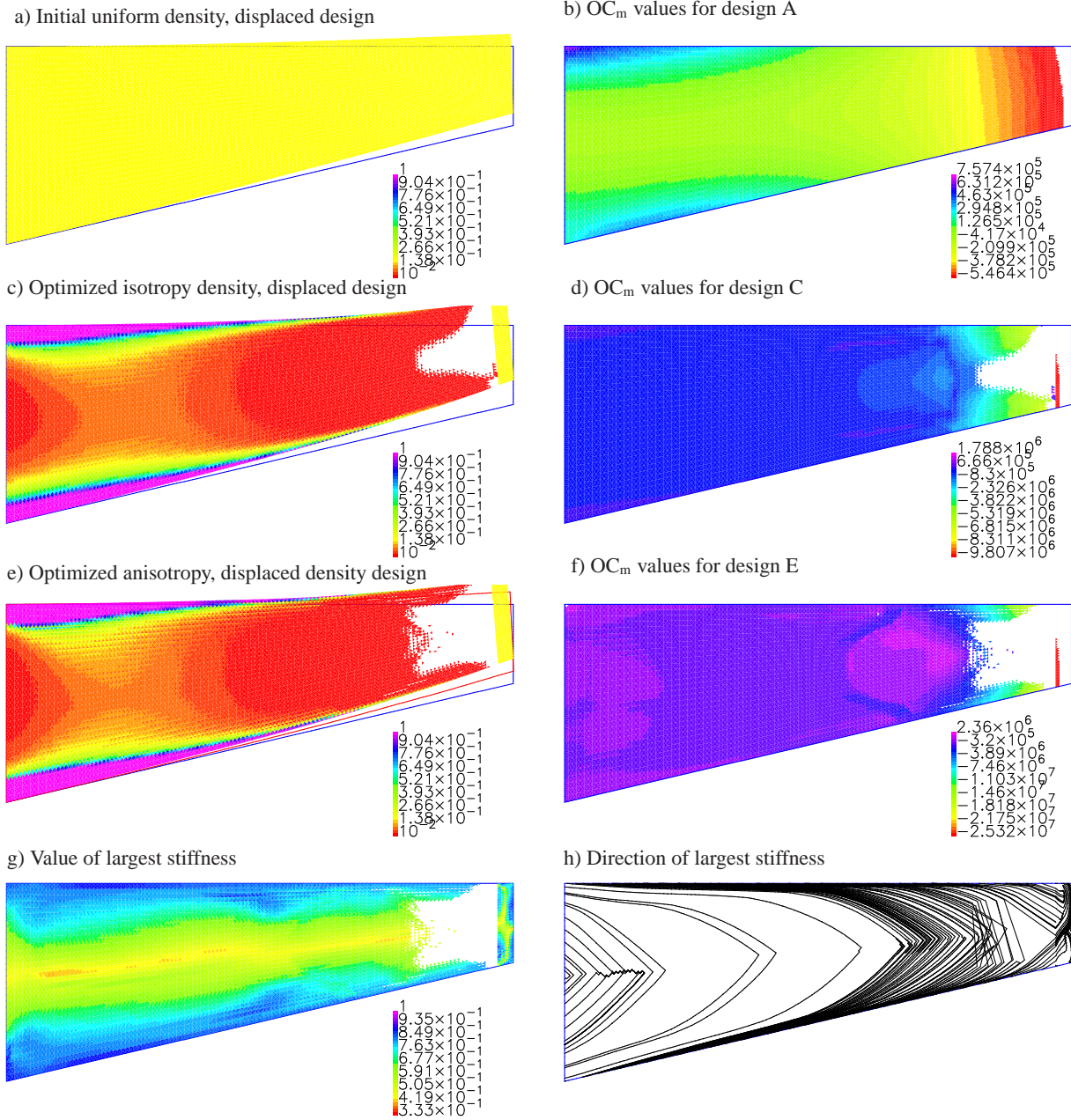


Fig. 3 Designs and responses for the cantilever problem with 20% of full material a) Initial uniform isotropic design with b) corresponding distribution of OC_m values — c) redesign after 10 isotropic density redesign with d) corresponding distribution of OC_m values — e) redesign after further 10 density redesign including anisotropy redesign with f) corresponding distribution of OC_m values — g) level of anisotropy resulting with h) showing directions of maximum stiffness.

almost constant in domains corresponding to active design parameters $\rho_{\min} < \rho_e < \rho_{\max}$. The white domains correspond to $\rho_e = \rho_{\min} = 0.01$, to be interpreted as holes.

After 10 more redesigns where the normalized constitutive matrices are also redesigned according to the simple formula (23) with modification (24) and the first eigenfrequency is increased further, now with a factor of 3.5. Figure 3e shows the optimized material distribution, being rather close to the distribution in 3c, meaning that the local constitutive redesign has only little influence on the optimized material distribution for this problem. Figure 3f shows the distribution of OC_m val-

ues for the optimized design in 3e. Also these OC_m values are almost constant in domains corresponding to active design parameters $\rho_{\min} < \rho_e < \rho_{\max}$ and the white domains correspond to $\rho_e = \rho_{\min} = 0.01$.

To illustrate the obtained anisotropy (in reality 6 components locally) Figure 3g shows a value for the level of anisotropy, being a number between 1/3 for isotropy and 1 for single directional "fiber", as explained in the appendix. The largest normalized stiffness is used to illustrate the level of anisotropy. Figure 3h shows lines of direction for the use of this largest normalized stiffness. Although not complete it is found that

the combination of Figures 3e, -g and -h give a rather good illustration of the final optimized design.

The shown histories in Figure 4 gives an impression of stable convergence for the chosen numerical procedure (14), with the same numerical control parameters 4.0, 0.8, $q = 0.8$ in (14) and $\beta = 0.2$ in (24) for all cases. For the 80% problem, the lower curve in Figure 4 for the third redesign is decreasing, meaning that the design changes has been too large. With the kept numerical control parameters it illustrates that the procedure (14)-(24) is able to repair a too large design change. Note, that the fixed tip amount of material is depending upon the total amount of material. The initial uniform designs imply the equal eigenfrequencies for all four cases.

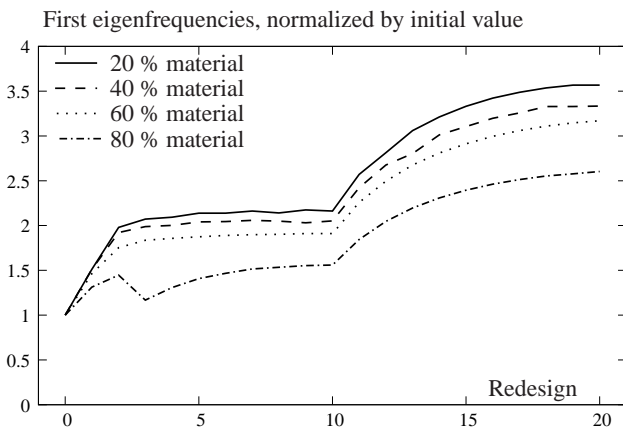


Fig. 4 Iteration histories for the cantilever problem with 20%, 40%, 60% and 80% material.

5.2 Beam-bridge with mode switching

Figure 5 shows the dimensions and data applied for this example. The mass and stiffness for this domain is thus different for the treated cases of 20%, 40%, 60% and 80% of full material, but without influence on the response of the initial uniform designs. The specific FE model has 28416 elements ($222 \times 32 \times 4$) and 16706 dof.

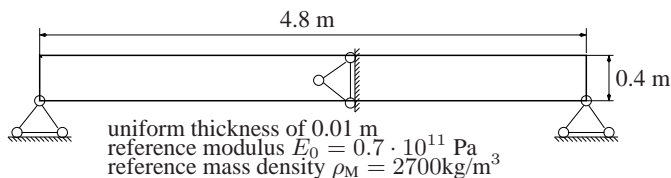


Fig. 5 Data for the beam-bridge problem with mode switching. Only midpoint supported in beam length direction.

Figure 6 shows the history of not only the first eigenfrequency but also the two closest eigenfrequencies obtained by subspace iteration. Almost multiple solutions are obtained and including mode switching. For the initial design the first

eigenmode is a bending mode as shown in Figure 7 which is also the case after only material density optimized, for the final optimized design the eigenmode is a longitudinal mode. This mode switching is due to the constitutive anisotropy design.

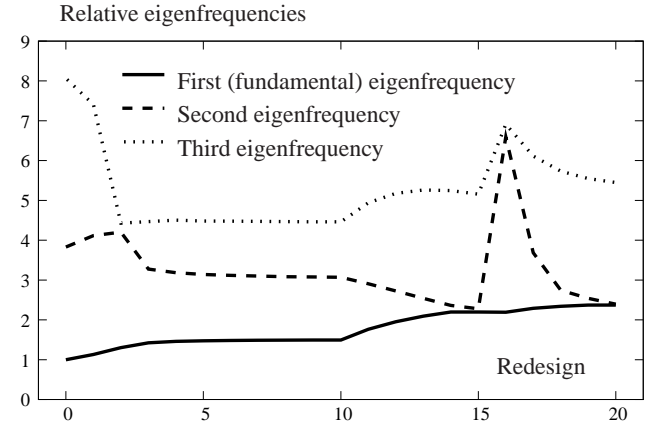


Fig. 6 Iteration histories for the beam-bridge problem with 20% material. Only anisotropy redesign from redesign number 10.

Note to Figure 6: Close to redesign step 2 eigenmodes 2 and 3 switch, close to redesign step 15 eigenmodes 1 and 2 switch, close to redesign step 16 possible multiple eigenmodes switch, and finally close to redesign step 20 eigenmodes 1 and 2 switch. Although multiple eigenfrequencies are involved a monotone increasing of the first eigenfrequency is found by the OC procedures.

With focus on the case of 20% material Figure 7 is a presentation similar to Figure 3 for the cantilever problem. The initial design, illustrated in Figure 7a is uniform material density (here ρ_e all equal to 0.2). Figure 7b shows the distribution of values of optimality criterion for material distribution OC_m for the initial design in 7a. The positive as well as negative values illustrate that a better material distribution can be obtained by redesign. After 10 redesigns of only material density, the first eigenfrequency is increased with a factor close to 1.5, and Figure 7c shows the optimized material distribution, when isotropy is kept. Figure 7d shows the distribution of OC_m values for the optimized design in 7c. Note, that these OC_m values are almost constant in domains corresponding to active design parameters $\rho_{\min} < \rho_e < \rho_{\max}$. The white domains correspond to $\rho_e = \rho_{\min} = 0.01$, to be interpreted as holes.

After 10 more redesigns where the normalized constitutive matrices are also redesigned according to the simple formula (23) with modification (24) the first eigenfrequency is increased further, now with a factor of 2.4. Figure 7e shows the optimized material distribution and is related to a longitudinal eigenmode. Figure 7f shows the distribution of OC_m values for the optimized design in 7e. Also these OC_m values are almost constant in domains corresponding to active design parameters $\rho_{\min} < \rho_e < \rho_{\max}$ and the white domains correspond to $\rho_e = \rho_{\min} = 0.01$. To illustrate the obtained anisotropy (in reality 6 components locally) Figure 7g shows

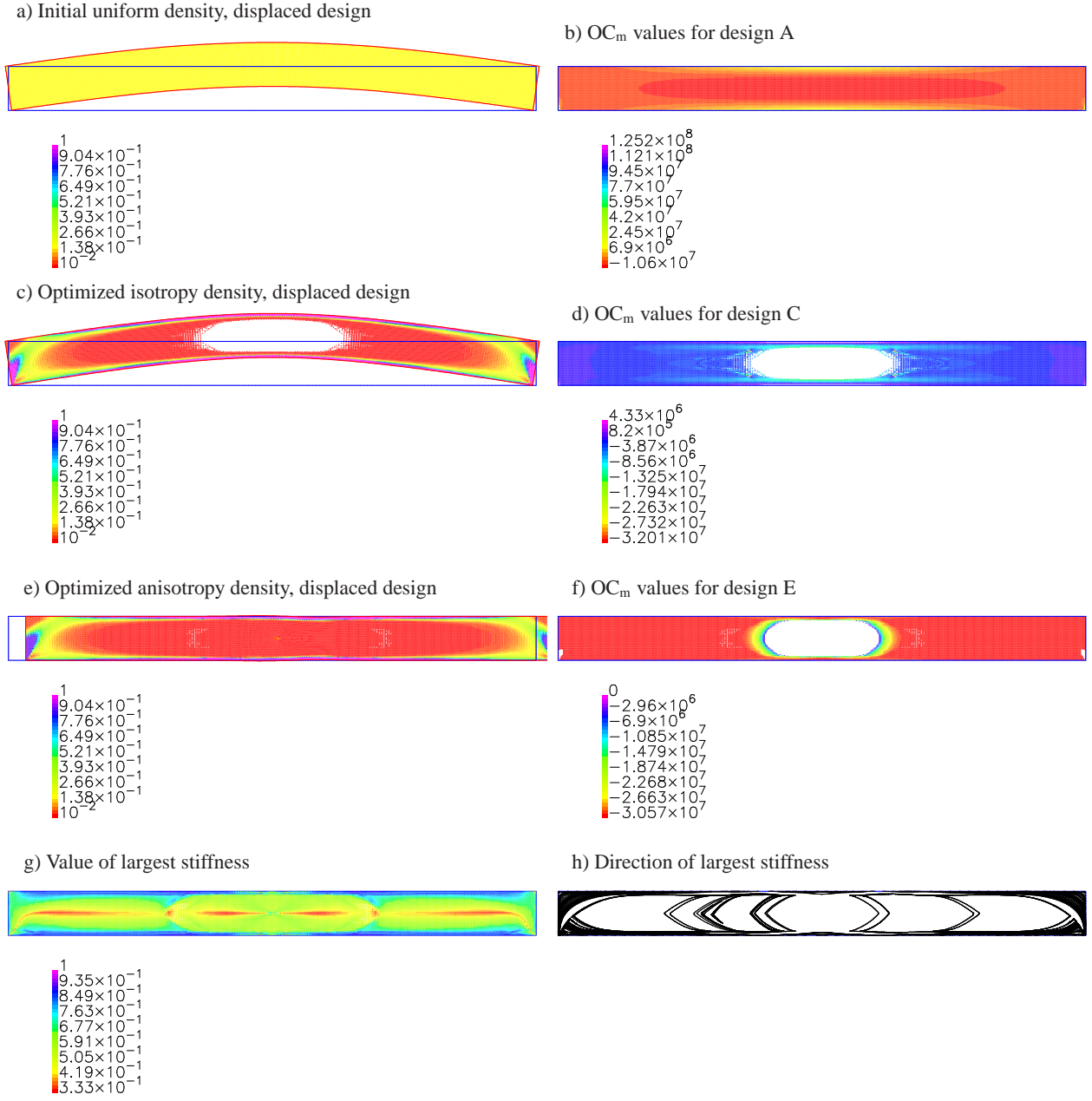


Fig. 7 Designs and responses for the cantilever problem with 20% of full material a) Initial uniform isotropic design with b) corresponding distribution of OC_m values — c) redesign after 10 isotropic density redesign with d) corresponding distribution of OC_m values — e) redesign after further 10 density redesign including anisotropy redesign with f) corresponding distribution of OC_m values — g) level of anisotropy resulting with h) showing directions of maximum stiffness.

values for the level of anisotropy, being a number between $1/3$ for isotropy and 1 for single directional "fiber". As explained in the appendix, the largest normalized stiffness is used to illustrate the level of anisotropy. Figure 7h shows lines of direction for the use of this largest normalized stiffness. Figures 7e, -g and -h give a rather good illustration of the final optimized design.

The shown iteration histories in Figure 8 gives an impression of stable convergence for the chosen numerical procedure (14), with the same numerical control parameters 4.0 , 0.8 , and $q = 0.8$ in (14) and $\beta = 0.2$ in (24) for all cases. With no

fixed design domain, it may be concluded that not only relative but also the absolute largest eigenfrequency is obtained for the smallest amount of material, not unexpected with the larger design possibilities.

6 Conclusion

While many papers in the literature present eigenfrequency optimized by material distribution, examples with eigenfre-

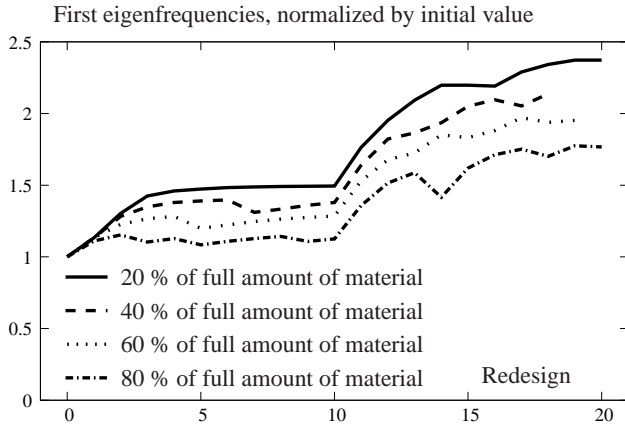


Fig. 8 Iteration histories for the beam-bridge problem with 20%, 40%, 60% and 80% of full material.

quency optimization by design of constitutive matrices does not seem available in the literature. The combined problem may be termed eigenfrequency optimization by free material optimization (FMO). In the present paper the essential point for a practical formulation is the separation of anisotropy description from the material distribution.

Local non-dimensional constitutive matrices are constrained to have unit norm of trace and Frobenius. An optimality criterion based on this constraint and stationary eigenfrequency shows that the components of a constitutive matrix are obtained directly from the strain state corresponding to the actual eigenmode. From this follows almost directly that the trace norm is equal to the Frobenius norm, which then may be scaled to unity. The amount of material is the material constraint for the combined optimization.

For the determination of material distribution among the elements of the model, a rather simplified optimality criterion is derived. Size constraints are satisfied iteratively with the amount of material completely satisfied in each iteration. The heuristic procedure for this shows good stability and rapid convergence. The explicit expression for the gradients of eigenfrequency as a function of local material density may at first seem complicated. They are shown to be extremely simple and general, which is believed to be a further major result in the present paper. Proportionality between element stiffness and material density is assumed in the present derivation, but a non-linear interpolation function will only modify the present results slightly, see Pedersen and Pedersen (2012). The resulting simple formula is a product of terms with direct physical interpretation. To clarify the derivation of this formula, a notation for partial derivation in combination with application of the chain rule is applied.

For the two examples with each four different amount of material, rather monotone increasing of the first eigenfrequency by redesign is observed. This includes cases of mode switching and multiple (close to multiple) eigenfrequencies. For these cases alternative formulations, such as objective by sum of eigenfrequencies, is not attempted. Simplicity is preferred, and the method of subspace for determination of several eigenmodes with close or equal eigenfrequencies, is an

essential part for problem-free optimization, using the present simple optimality criteria approach.

References

- Grandhi, R. (1993). Structural optimization with frequency constraints - a review. *AIAA Journal* 31(12):2296–2303.
- Jacobi, C. G. J. (1846). Über ein leichtes verfahren die in der theorie der secularstörungen vorkommenden gleichungen numerischen aufzulösen. *Crelle's journal* 30:51–95.
- Niordson, F. I. (1965). On the optimal design of a vibrating beam. *Quarterly of Applied Mathematics* 23:47–53.
- Pedersen, P., and Pedersen, N. L. (2005). An optimality criterion for shape optimization in eigenfrequency problems. *Struct. Multidisc. Optim.* 29(6):457–469.
- Pedersen, P., and Pedersen, N. L. (2012). Interpolation/penalization applied for strength designs of 3d thermoelastic structures. *Struct. Multidisc. Optim.* 45:773–786.
- Pedersen, P., and Pedersen, N. L. (2013). On strength design using free material subjected to multiple load cases. *Struct. Multidisc. Optim.* 47(1):7–17.
- Stingl, M., Kocvara, M., and Leugering, G. (2009). Free material optimization with fundamental eigenfrequency constraints. *SIAM J. Optim.* 20(1):524–547.
- Wittrick, W. H. (1962). Rates of change of eigenvalues, with reference to buckling and vibration problems. *J. Royal Aeronautical Soc.* 66:590–591.

A

Direction of largest longitudinal material stiffness

For illustration of the optimized designs the distributions of material density has been shown. However, for anisotropic material the anisotropy should also be illustrated, but without going into detail of the six components $\tilde{L}_{1111}, \tilde{L}_{2222}, \tilde{L}_{1212}, \tilde{L}_{1122}, \tilde{L}_{1112}, \tilde{L}_{2212}$ given in the global x, y coordinate system. It is chosen to show a plot of the directions of largest longitudinal material stiffness.

According to laminate theory \tilde{L}_{1111} as a function of rotation, termed $f(\theta)$, is given by the six components in the x, y coordinate system

$$f(\theta) = (\tilde{L}_{1111} + \tilde{L}_{2222})/2 + \tilde{L}_2 \cos(2\theta) - \tilde{L}_3(1 - \cos(4\theta)) + \tilde{L}_6 \sin(2\theta) + \tilde{L}_7 \sin(4\theta) \quad (25)$$

where the practical parameters are defined by

$$\begin{aligned} \tilde{L}_2 &= (\tilde{L}_{1111} - \tilde{L}_{2222})/2 \\ \tilde{L}_3 &= (\tilde{L}_{1111} + \tilde{L}_{2222} - 2(\tilde{L}_{1122} + 2\tilde{L}_{1212}))/8 \\ \tilde{L}_6 &= (\tilde{L}_{1112} + \tilde{L}_{2212})/2 \\ \tilde{L}_7 &= (\tilde{L}_{1112} - \tilde{L}_{2212})/2 \end{aligned} \quad (26)$$

For orthotropic materials $\tilde{L}_6 = \tilde{L}_7 = 0$ in specific directions, but for the free material subjected to multiple load cases this will not always be the case, so we need to analyze the more complicated material. More extremum solutions for $f(\theta)$ exist in the actual interval of $0 \leq \theta < \pi$. To locate the maximum of $f(\theta)$ it is therefore decided to evaluate (25) at a number of θ values (here chosen with increments $\Delta\theta = \pi/1800$). This has been done for each elements.

A.1

Levels of anisotropy

Lines for direction of largest longitudinal material stiffness in addition to the color scale for distribution of material density give some physical information about the optimized material, but not much about the level of local anisotropy. Improved information is obtained by adding a color scale for the value of the larger longitudinal stiffness, i.e., the maximum of $f(\theta)$ found in determining the directions θ .

The values of f_{\max} has an upper bound of 1 and a lower bound of $1/3$. This follows from the trace being 1, and thus having eigenvalues in this interval. This then also follows for the non-dimensional longitudinal stiffness. For higher values of f_{\max} a single fiber direction is approached and for lower values of f_{\max} an isotropic material with zero Poisson's ratio material is approached.